Metamorphic diamonds: Mechanism of growth and inclusion of oxides

Data · January 2001

DOI: 10.1130/0091-7613(2001)029<0263:MDMOGA>2.0.CO;2

Larissa Dobrzhinetskaya
University of California, Riverside

Downloaded from geology.gsapubs.org on 7 February 2009

Geology

Metamorphic diamonds: Mechanism of growth and inclusion of oxides

L.F. Dobrzhinetskaya, H.W. Green, II, T.E. Mitchell and R.M. Dickerson

Geology 2001;29;263-266
doi:10.1130/0091-7613(2001)029<0263:MDMOGA>2.0.CO;2

E-mail alerting services	click www.gsapubs.org/cgi/alerts to receive free e-mail alerts when new articles cite this article
Subscribe	click www.gsapubs.org/subscriptions/index.ac.dtl to subscribe to Geology
Permission request	click http://www.geosociety.org/pubs/copyrt.htm#gsa to contact GSA

Copyright not claimed on content prepared wholly by U.S. government employees within scope of their employment. Individual scientists are hereby granted permission, without fees or further requests to GSA, to use a single figure, a single table, and/or a brief paragraph of text in subsequent works and to make unlimited copies of items in GSA's journals for noncommercial use in classrooms to further education and science. This file may not be posted to any Web site, but authors may post the abstracts only of their articles on their own or their organization's Web site providing the posting includes a reference to the article's full citation. GSA provides this and other forums for the presentation of diverse opinions and positions by scientists worldwide, regardless of their race, citizenship, gender, religion, or political viewpoint. Opinions presented in this publication do not reflect official positions of the Society.

Notes

© 2001 Geological Society of America

THE
GEOLOGICAL
SOCIETY
OF AMERICA

Metamorphic diamonds: Mechanism of growth and inclusion of oxides

L.F. Dobrzhinetskaya
H.W. Green II
Institute of Geophysics and Planetary Physics, University of California, Riverside, California 92521, USA
T.E. Mitchell
R.M. Dickerson
Center for Materials Science, Los Alamos National Laboratory, Los Alamos, New Mexico 87545, USA

ABSTRACT

We report a detailed series of electron microscope observations of metamorphic microdiamonds included in and separated from garnets and zircons from a single specimen of garnet-biotite-feldspar gneiss from the Kokchetav massif, Kazakhstan. The morphology of the diamonds ranges from skeletal forms composed of thin {111} plates through cuboid and octahedral forms. Included within the diamonds is a diverse suite of nanometric oxides, suggesting that the C-O-H fluid from which the diamonds grew may have carried chemical components derived from both the sediments and the mantle. The spectrum of morphologies and their abundant tiny inclusions can all be explained by a simple model based on the ratio of the rate at which {111} plates grow and the rate of random nucleation of new plates at their edges.

Keywords: diamonds, inclusions, oxides, eskolaite, magnesite, mechanism, crystal growth.

INTRODUCTION

The discovery of microdiamonds within metamorphosed rocks of continental affinity (Kazakhstan, China, Norway, and Germany) and their subsequent study have revolutionized our understanding of continental collision zones and the processes of subduction and exhumation (Rozen et al., 1972; Sobolev and Shatsky, 1990; Xu et al., 1992; Dobrzhinetskaya et al., 1995; De Corte et al., 1998, 2000; Nasdala and Massonne, 2000). The site of the original discovery, the Kokchetav massif, is situated in the northern part of Kazakhstan. More than 90% of the diamondiferous metamorphic rocks of the massif are represented by feldspathic gneiss and quartz-rich rocks, although diamonds also occur in garnet pyroxenite and calc-silicate rocks. These rocks formed as sediments at Earth's surface and subsequently underwent metamorphism at a minimum pressure of 3.5–4 GPa and temperature of ~900–1100 °C (Zhang et al., 1997) at ≥120 km depth during continental collision ca. 520–540 Ma (Claoue-Long et al., 1991). The diamonds (10–100 μm diameter) occur as inclusions in garnet, quartz, biotite, phlogopite, diopside, kyanite, and zircon as well as at grain boundaries, even though many of these minerals are unstable under conditions of diamond formation. The lower pressure overprint represented by quartz and the hydrous minerals occurred at perhaps 500–700 °C and resulted in partial replacement of diamond by graphite.

The mechanisms and conditions of growth of these microdiamonds are still poorly understood, although growth from a C-O-H fluid is strongly implied by the infrared spectroscopic results of De Corte et al. (1998, 2000). These authors also showed lithology-specific diamond populations distinguished by color, morphology, nitrogen concentration, and δ^{13}C values. Shatsky et al. (2000) showed that many of these morphologies are also displayed by microdiamonds from Siberian kimberlite pipes. However, Katayama et al. (1998) showed evidence for solid-state transformation of graphite to diamond in a single inclusion in zircon.

Here we focus on a single specimen of garnet-biotite gneiss that records diverse morphologies of microdiamonds, a rich inclusion suite of oxides, and graphitization and alteration during exhumation. We examined diamonds in situ (i.e., included in garnet and zircon) as well as diamonds extracted from garnets. The systematic variations across the large spectrum of morphologies observed lead us to a simple model of diamond growth that explains the diversity of forms and the abundance of nanometric inclusions.

METHODS

Specimen #K-123/93 of garnet-biotite quartzofeldspathic gneiss was collected from an outcrop at the northeast shore of Lake Kumdikol. This specimen also contains graphite, calcite, and chlorite; tourmaline and sphene are accessory minerals. Wet chemical analysis of the bulk rock yielded (wt%): SiO_2 = 53.26, Al_2O_3 = 17.14, Fe_2O_3 = 8.61, TiO_2 = 1.09, MgO = 3.37, CaO = 5.93, Na_2O = 3.04, K_2O = 3.09, MnO = 0.13, Cr_2O_3 = 0.00, P_2O_5 = 0.35, loss = 3.73; sum = 99.73. Garnet composition determined by Cameca SX-50 EMMA is (wt%): SiO_2 = 38.26, Al_2O_3 = 21.05, Fe_2O_3 = 21.48, TiO_2 = 0.26, MgO = 7.33, CaO = 11.04, Na_2O = 0.07, K_2O = 0.01, MnO = 0.13, Cr_2O_3 = 0.00; Sum = 99.63.

Diamonds were prepared by zircon and garnet separation. We separated ~5 mg of zircons from 10 kg of rock by standard electromagnetic and heavy-liquid separation and hand-picking under the optical microscope. Selected zircons were mounted on glass slides and polished using a slurry of 0.06 μm colloidal SiO_2 at high pH. Garnet separation involved thick polished sections (50–70 μm) prepared with Crystalbond as a mounting medium. Examination with an EDGE microscope identified individual garnets containing 25–50 microdiamonds each. The sections were removed from the glass, gently crushed, and the garnets were hand-picked. The resulting clean garnet concentrate was ground to a particle size of 30–50 μm in an agate mortar and immersed in reagent-grade HF for 7 days, after which diamonds 5–30 μm diameter were separated by rinsing and centrifugation in H_2O and ultrasonic cleaning. Both the diamonds isolated from garnets and the polished diamond-containing zircons were examined by scanning electron microscope (SEM; Philips XL30 FEG). Transmission electron microscope (TEM) foils were prepared from 10 skeletal and 3 cuboid-octahedral diamonds (Alani et al., 1997) and observed in a Philips CM300 and JEOL 3000F.

Geology; March 2001; v. 29; no. 3; p. 263–266; 3 figures.

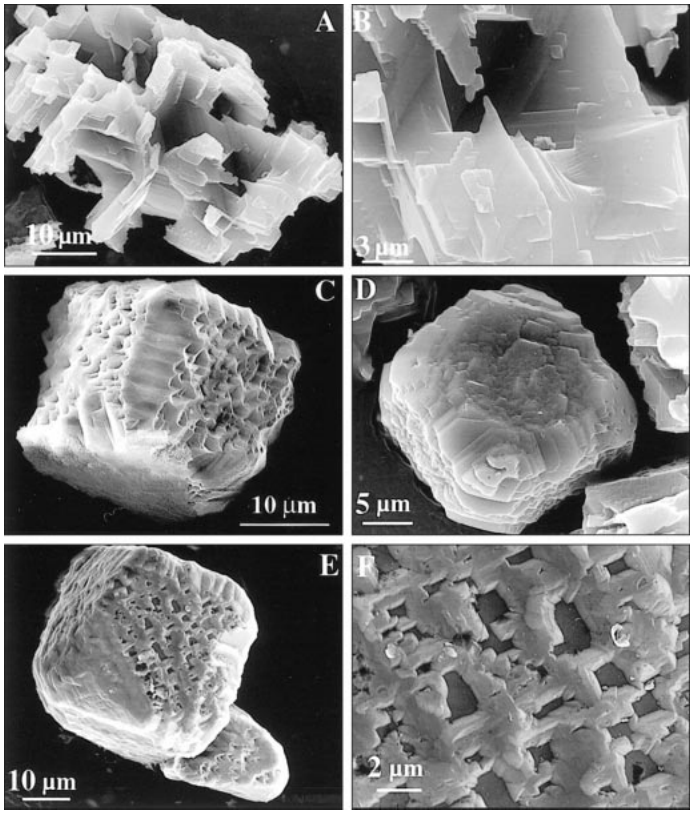

Figure 1. Scanning electron microscope images of diamonds separated from garnet. A, B: Skeletal crystals with house of cards morphology. C: Cuboid crystal with antiskeletal cavities on cuboid surfaces. D: Cuboid-octahedron with abundant small {111} facets on cuboid faces. E: Cuboid-octahedron with graphite-filled cavities exposed on cuboid faces. F: Detail of crystal shown in E.

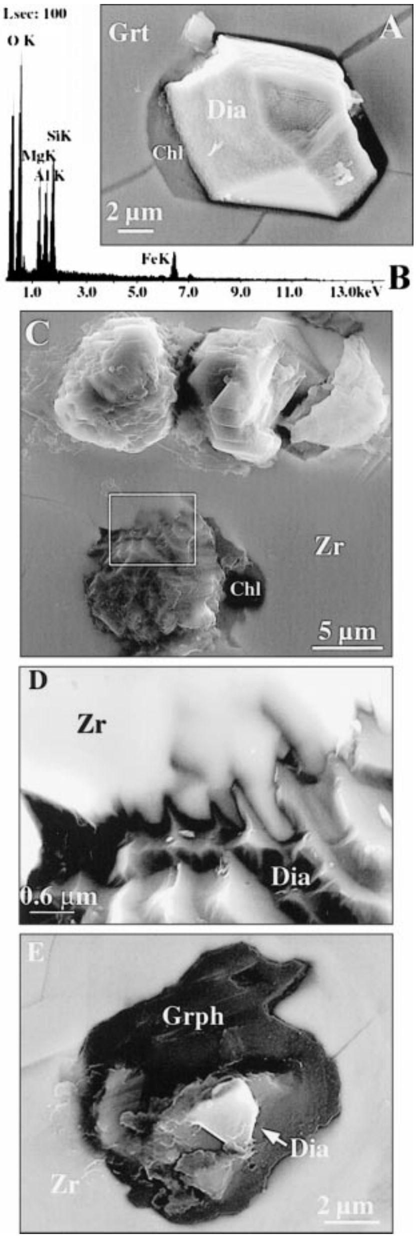

Figure 2. Scanning electron microscope images of diamonds included in slightly zoned garnet (Grt, A, B) and in homogeneous, unzoned zircon (C–E). A: Deep triangular pit on exposed {111} surface and traces of natural etching visible on curved diamond (dia) faces; this diamond, surrounded by secondary chlorite (Chl), is situated in central part of host garnet, which is characterized by higher CaO (8.03 wt%) and lower MgO (8.72 wt%) and FeO (20.26 wt%) in comparison with rim (in wt%: CaO = 7.69; MgO = 8.87; FeO = 20.47). B: Energy-dispersive spectrum of chlorite. C: Five diamond inclusions, three of them rose-like—one well-exposed (center of linear group), one just emerging (top), and other (bottom) partly surrounded by secondary chlorite. Zr is zircon. D: Detail of diamond-zircon interface of framed area in C showing sharp edges of rose petals. E: Graphitized diamond in zircon; core of inclusion is still diamond surrounded by thick graphite (graph) rim.

RESULTS

A selection of microdiamonds separated from garnets was spread on a glass slide and a region was randomly chosen for counting. The 156 diamonds were classified as: (1) skeletal (62.40%); (2) cuboid-octahedron (36.32%; no pure end members were observed); and (3) irregular forms (58.37%). Representative examples of types 1 and 2 are shown in Figure 1. Skeletal forms are dominated by {111} plates assembled into a house of cards morphology (Fig. 1, A and B). These forms grade into antiskeletal crystals approximating cubic habit (cf. De Corte et al., 2000; Shatsky et al., 2000) with octahedral facets on their corners and along their edges and large numbers of octahedrally faceted cavities in their roughly {100} surfaces (Fig. 1C). Fully dense crystals also exhibit cuboid-octahedral habit, generally with larger {111} facets (Fig. 1, D–F). Note that the cuboid surfaces of C and D in Figure 1 show no {100} facets per se. Instead, cuboid surfaces consist of myriad small facets of variable size representing all four orientations of {111}. In rare cases, the cavities on cuboid faces of antiskeletal crystals are filled by graphite (Fig. 1, E and F). The faceted boundaries of the graphite-filled channels exposed on the cuboid face of E and F in Figure 1 are parallel to octahedral faces, yielding channel margins parallel to <110> directions. Cavity boundaries intersecting cuboid surfaces parallel to <110> also can be seen on the left-facing surface of Figure 1C. Among the irregular forms, rose crystals, in which one orientation of octahedral faces dominates, are common (not shown).

Identifiable evidence of etching such as curved faces and trigonal etch pits is rare. Figure 2A shows a two-phase inclusion in garnet. The surfaces of both phases are curved and irregular, except for the octahedral facet on top of the diamond that contains a deep triangular pit. The dark phase surrounding the diamond is chlorite (energy dispersive spectrum [EDS] is shown in Fig. 2B; identification confirmed by wavelength-dispersive spectroscopy [WDS]). Chlorite also occurs around etched diamonds in zircon (Fig. 2C) and cracks filled with similar material radiate from other altered inclusions.

The same variability of shapes exhibited by diamonds observed in and extracted from garnets is observed for inclusions in zircon. Figure 2C shows five diamonds in a single zircon. Note the rose-like shape of the diamond in the middle of the linear group of three and the similarity between the left-most diamond of that group and the cuboid-octahedron in Figure1D. More difficult to see in this image are the delicate and complicated borders of the two diamonds above and below the linear group and the small patches of chlorite. A detail (Fig. 2D) of the lowermost diamond in Figure 2C shows a diamond rose that has been faithfully enveloped by the growing zircon, preserving the sharp edges of the petals of the rose. In contrast to these perfectly preserved diamonds, partial or complete graphitization has occurred in others (Fig. 2E); in this case and many others, an extremely irregular interface with zircon suggests that they, too, were originally diamonds of skeletal or rose morphology.

Transmission electron microscope analysis of skeletal diamonds shows that they contain a wide variety of nanocrystalline oxides as well as carbonate and rare silicates. Although we have obtained energy dispersive spectra of the inclusions, because of their occurrence within diamonds formed at pressures in excess of 4 GPa; we need to establish their crystal structures by electron diffraction before we can confidently identify them. The possibility that some may represent high-pressure minerals holds the potential for defining more precisely the pressures to which these rocks have been subducted. Figure 3 provides a few representative images and energy dispersive spectra of such inclusions. Note that some are essentially pure phases (e.g., Fig. 3C), whereas others obviously have small components of other phases. We have successfully prepared foils from a restricted number of cuboid-octahedral microdiamonds for transmission electron microscope analysis (Alani et al., 1997), revealing dislocations and platelets but few solid inclusions. An exception within a fluid inclusion bounded by {111} crystal facets is shown in Figure 3E.

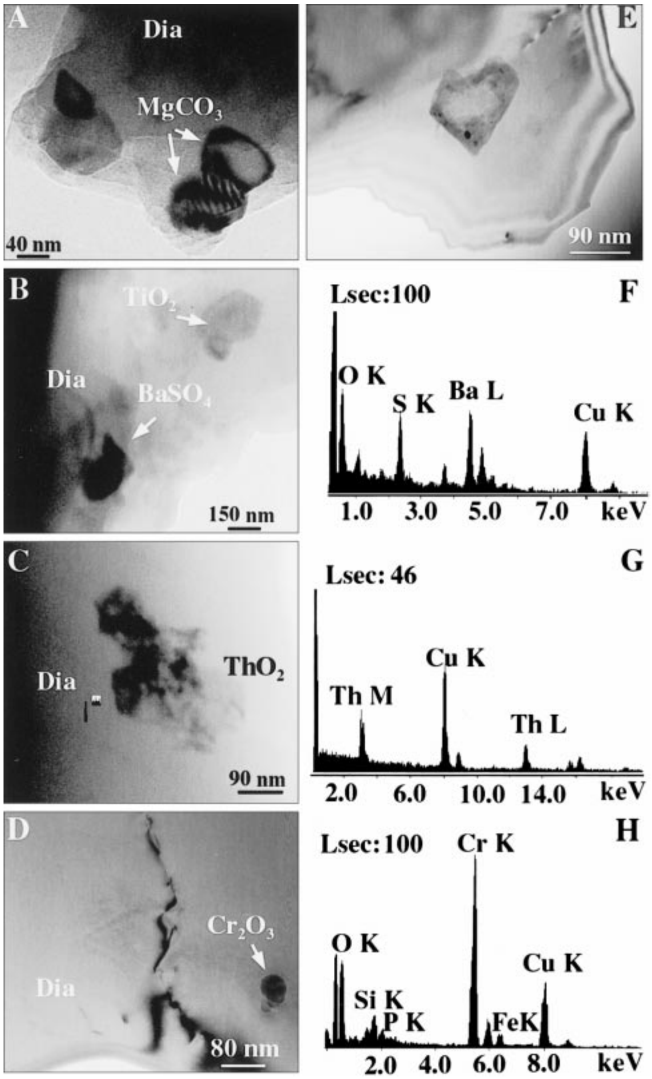

Figure 3. Transmission electron microscope images of diamonds with nanocrystalline inclusions. A: $MgCO_3$ (magnesite?). B: TiO_2 (rutile?) and $BaSO_4$ (barite?). C: ThO_2, D: Cr_2O_3 (eskolaite?). E: Negative crystal fluid inclusion with solid inclusions on its walls (note black spot near base of inclusion that is strongly diffracting electrons). F–H: Energy dispersive spectra of $BaSO_4$, ThO_2, and Cr_2O_3 (Cu peaks originate from support grids).

DISCUSSION

Irregular skeletal forms develop if atoms are added to the edges and corners of a growing crystal more rapidly than to the centers of crystal faces (e.g., Chernov, 1974). During rapid edge growth, internal cavities may develop on crystal faces, with the possibility of entrapment and preservation of the fluid from which the crystal grows. Our direct observations of skeletal crystals with myriads of partially formed cavities bounded by {111} planes (Fig. 1, A and B), of a single fully enclosed, faceted, cavity (Fig. 3E), and of diamonds with {111} bounded cavities open to cuboid surfaces (Fig. 1, C, E, and F), suggest that development of such cavities and their entrapment may have been common in growth of Kokchetav diamonds.

Diamond growth can be divided into three broad categories based upon the ratio of driving force for growth to reaction kinetics; Sunagawa (1990, 1997) identified three kinetic-morphologic fields, including a region at low driving force and/or rapid kinetics where highly perfect crystals grow, a region at high driving force and/or slow kinetics where highly imperfect growth is expected to occur, and a region in between, where hopper and/or skeletal crystals predominate. Sunagawa considered the kinetic effects to be due to temperature alone, but Kanda (1985) and Pal'yanov et al. (1999) showed that the fluid from which diamonds grow (H_2O and carbonate melt, respectively) can have an important additional effect on kinetics and hence on morphology (H_2O increases skeletal morphology and carbonate melt yields perfect octahedra). Thus, increasing the driving force for growth and decreasing the kinetics of growth have similar effects on diamond morphology, but the kinetics cannot be simply described in terms of temperature.

In the suite of diamonds reported here, only {111} crystal facets develop to any significant degree. Nevertheless, the morphological diversity ranges from skeletal varieties consisting only of {111} plates to fully dense cuboid crystals and octahedra. Moreover, transitional types between the major groups are also observed (e.g., antiskeletal cuboid forms, Fig. 1C). There is an underlying theme that suggests variations on a common mechanism of growth. We propose that all of these morphologies are a consequence of growth dominated by {111} platelets in which the morphology that develops in an individual crystal depends on the ratio between the rate at which new plates nucleate at the margins of existing plates (N) and the rate plates grow in their own plane (G). Variation of N/G has the following consequences.

1. If the ratio of new plate nucleation rate to in-plane growth rate is very small (N/G << 1), the result will be open skeletal forms consisting of large plates surrounding a wide variety of cavity sizes, some of significant size compared to the crystal as a whole, such as shown in Figure 1 (A and B). Progressively larger ratios of N/G will result in progressively smaller plate and cavity sizes.

2. If the nucleation of new octahedral plates along the edges of old plates is statistically random in space and time, and if N/G is moderate and is constant with time, symmetry constraints require that the macroscopic form of the crystal must show statistically cubic symmetry. Combining this constraint with the fact that {100} planes are furthest away in terms of orientation from the {111} planes that accomplish crystal growth, it follows that the hypothetical {100} faces that are approximated by cuboid surfaces are effectively the slowest growing and therefore dominate macroscopic form. The result, therefore, is development of cuboid forms with octahedral facets on their corners and along their edges, and with {111} bounded cavities in their irregular {100} surfaces, such as in Figure 1C (see also Fig. 3, d and e, of de Corte et al., 2000; Fig. 3b of Shatsky et al., 2000). The cavity boundaries will intersect in <110> directions, such as in Figure 1 (E and F). As N/G becomes larger, cavity sizes decrease and the morphology grades into fully dense cuboid crystals in which the irregular cuboid surfaces do not exhibit cavities, but nevertheless retain their <110> lineations defined by large numbers of intersecting small {111} facets, such as in Figure 1D.

3. In the limit as nucleation of new {111} plates becomes greatly dominant over plate growth (N/G >> 1), the barrier to nucleation of new layers on existing plates is removed and the concept of plate growth becomes meaningless; normal crystal growth then proceeds in which crystal habit is controlled by the inherent differences in growth rate of different forms. As a consequence, {111} faces will dominate at all times, internal cavities will not form, and octahedral habit will be observed.

Observation in this single rock specimen of almost the full spectrum of forms to be expected from kinetically controlled platelet growth underlines kinetic control of morphology. The Sunagawa model would predict that the temperature changed significantly during the course of diamond mineralization or that the degree of supersaturation of the fluid in carbon changed greatly. The additional observations of Kanda (1985) and Pol'yanov et al. (1999) suggest, however, that the composition of the fluid could have changed in other ways. Late graphite growth in cavities records change of temperature (or pressure) during diamond growth; the observation of widely different solid inclusions in diamonds also shows at least local variation in fluid composition.

Our model, as presented, presumes that N/G remained constant through the growth of individual crystals. Alternatively, if N/G should increase during growth of an individual crystal, an evolution of forms from skeletal through cuboid to octahedral habit could occur. The infilling of cavities on cuboid surfaces by graphite is evidence for such change in growth habit upon return of the rock to the graphite stability field. Similar infilling by diamond could have occurred in other diamonds and would escape detection unless there is some memory preserved in the diamond of the former growth mode. Early skeletal growth followed by bulk growth is consistent with cathodoluminescent images of diamond plates from Yakutian microdiamonds containing cores of skeletal and cuboid forms (see Fig. 8, b and d, of Shatsky et al., 2000). It would not be unreasonable for infilling carbon to have a different isotopic composition from initial carbon, hence it might be possible to find diamonds with intricately intertwined isotopic microdomains, reflecting such infilling.

A corollary of our model is that the diamonds grew from a fluid that originally filled the void spaces and precipitated the nanocrystalline oxides, each perhaps in its unique microchemical environment largely isolated from that of others. Whereas $BaSO_4$ and ThO_2 suggest continental affinity and probably have their source in the host rocks of sedimentary origin, Cr_2O_3 is potentially an indicator of a component imported from the mantle. Further investigations should allow stronger statements to be made about whether clearly external components are present and, if so, whether they are rare or common. Given the diversity of the inclusions in individual diamonds, it seems unlikely that these inclusions formed in global equilibrium with the mineralogy of the rock; they more likely formed in isolated microenvironments within cavities in the diamonds. The inclusion-bearing cavity shown in Figure 3E supports this view.

In summary, our results amplify and extend the findings of De Corte et al. (1998, 2000). We show an image of an entrapped cavity of the sort they inferred and we directly identify magnesite within the diamonds, as well as a diverse population of oxide inclusions, strongly supporting their spectroscopic evidence for growth from a hydrous fluid. This fluid was sufficiently enriched with oxygen to produce oxidized species, including $MgCO_3$ (recorded also as carbonate and water in microdiamonds from Kumdikool garnet pyroxenites; De Corte et al., 2000), but it was not high enough to oxidize diamond. CH_4 and other reduced species have not been reported in any Kokchetav diamonds. The diversity of solid inclusions suggests that this fluid may have carried both crustal and mantle components. The variety of diamond forms preserved in this single rock specimen is consistent with a simple growth model that explains both the spectrum of forms observed and the abundance and diversity of nanometric inclusions. Based upon the similarities between Kokchetav and Yakutian microdiamonds (Shatsky et al., 2000), our growth model may also hold for other types of microdiamonds.

ACKNOWLEDGMENTS

We thank K. Bennett, L. Jakobson, C. Keller, and K. Bozhilov for interesting discussions. This project was partially supported by a grant from Los Alamos National Laboratory (no. 9949 to Dobrzhinetskaya). G. Ernst, T.E. McCandless, and P. Cartigny provided constructive comments that helped to improve the manuscript.

REFERENCES CITED

Alani, R., Dobrzhinetskaya, L., Green, H., and Mitchell, T., 1997, Metamorphic microdiamond: A specific technique for TEM foil preparation: Eos (Transactions, American Geophysical Union), v. 78, p. 738.

Chernov, A.A., 1974, Stability of faceted shapes: Journal of Crystal Growth, v. 24/25, p. 11–31.

Claoue-Long, J.C., Sobolev, N., Shatsky, V., and Sobolev, A., 1991, Zircon response to diamond-pressure metamorphism in the Kokchetav massif, USSR: Geology, v. 19, p. 710–713.

De Corte, K., Cartigny, P., Shatsky, V., Sobolev, N., and Javoy, M., 1998, Evidence of fluid inclusions in metamorphic microdiamonds from the Kokchetav massif, northern Kazakhstan: Geochimica et Cosmochimica Acta, v. 62, p. 3765–3773.

De Corte, K., Cartigny, P., Shatsky, V., De Paepe, P., Sobolev, N.V., and Yavoy, M., 2000, Characteristics of microdiamonds from UHPM rocks of the Kokchetav massif (Kazakhstan), *in* Gurney, J.J., et al., eds., Proceedings of the VIIth International Kimberlitic Conference: Cape Town, South Africa, Red Roof Design cc, p. 174–182.

Dobrzhinetskaya, L., Eide, E., Korneliussen, A., Larsen, R., Millege, J., Posukhova, T., Smith, D.S., Sturt, B., Taylor, W.R., and Tronnes, R., 1995, Diamond in metamorphic rocks of the Western Gneiss region in Norway: Geology, v. 23, p. 597–600.

Kanda, H., 1985, Effect of metal and water on growth and dissolution morphologies of diamond crystals [thesis]: Sendai, Japan, Tohoku University, 137 p.

Katayama, I., Zayachkovsky, A., and Maruyama, S., 1998, A window to prograde metamorphism of the Kokchetav massif, northern Kazakhstan, *in* International workshop on UHP metamorphism and exhumation, Abstracts: Stanford, California, Stanford University, p. 91–95.

Nasdala, L., and Massonne, H.-J., 2000, Microdiamonds from the Saxonian Erzgebirge, Germany: In situ micro-Raman characterization: European Journal of Mineralogy, v. 12, p. 495–498.

Pal'yanov, Y., Sokol, A., Borzdov, Y., Khokhryakov, A., and Sobolev, N., 1999, Diamond formation from mantle carbonate fluids: Nature, v. 400, p. 417–418.

Rozen, O., Zorin, Y., and Zayachkovsky, A., 1972, A find of the diamonds within eclogites of the Precambrian Kokchetav massif: Doklady Academii Nauk SSSR, v. 203, p. 674–676.

Shatsky, V., Zedgenizov, E., Yefimova, E., Rylov, G., De Corte, K., and Sobolev, N., 2000, A comparison of morphology and physical properties of microdiamonds from the mantle and crustal environments, *in* Gurney, J.J., et al., eds., Proceedings of the VIIth International Kimberlitic Conference: Cape Town, Africa, Red Roof Design cc, p. 757–763.

Sobolev, N., and Shatsky, V., 1990, Diamond inclusions in garnets from metamorphic rocks: A new environment of diamond formation: Nature, v. 343, p. 742–746.

Sunagawa, I., 1990, Growth and morphology of diamond crystals under stable and metastable conditions: Journal of Crystal Growth, v. 99, p. 156–1161.

Sunagawa, I., 1997, Natural crystallization: Journal of Crystal Growth, v. 42, p. 214–223.

Xu, S., Okay, A.I., Sengor, A., Su, W., Liu, Y., and Jiang, L., 1992, Diamond from the Dabie Shan metamorphic rocks and its implication for tectonic setting: Science, v. 256, p. 80–82.

Zhang, R.Y., Liou, J.G., Ernst, W.G., Coleman, R.G., Sobolev, N., and Shatsky, V., 1997, Petrological characteristics and metamorphic evolution of diamond-bearing and associated rocks from the Kokchetav massif, northern Kazakhstan: Journal of Metamorphic Geology, v. 15, p. 479–496.

Manuscript received July 24, 2000
Revised manuscript received November 9, 2000
Manuscript accepted November 29, 2000

Printed in USA